Vol 17 No 2, February 2008
1674-1056/2008/17(02)/0726-10
Chinese Physics B
© 2008 Chin. Phys. Soc.
and IOP Publishing Ltd

Theoretical study of the trapping efficiency of an optical tweezers array system*

Li Qin(李 勤)[a)†], Feng Wan-Li(冯万力)[b)], Hu Xiao-Ming(胡晓明)[a)],
Cao Qun(曹 群)[a)], Sha Ding-Guo(沙定国)[b)], and Lin Jia-Ming(林家明)[b)]

[a)] *Department of Biomedical Engineering, Beijing Institute of Technology, Beijing* 100081, *China*

[b)] *Department of Opto-electronic Engineering, Beijing Institute of Technology, Beijing* 100081, *China*

(Received 11 May 2007; revised manuscript received 23 August 2007)

Optical tweezers have been a valuable research tool since their invention in the 1980s. One of the most important developments in optical tweezers in recent years is the creation of two-dimensional arrays of optical traps. In this paper, a method based on interference is discussed to form gradient laser fields, which may cause the spatial modulation of particle concentration. The parameters related to the optical tweezers array are discussed in detail and simulated by the Matlab software to show the influence of important parameters on the distribution of particle concentration. The spatial redistribution of particles in a laser interference field can also be predicted according to the theoretical analysis.

Keywords: optical tweezers array, gradient force, trapping efficiency, spatial modulation
PACC: 8754

1. Introduction

During the last decades, 'optical tweezers array' systems have been extensively investigated from both theoretically and experimentally. Since Ashkin *et al*[1] demonstrated the trapping of a microscopic dielectric particle by a three-dimensional optical gradient force, optical tweezers have been used in a wide range of applications. The optical tweezers use the mechanical action of the laser beam to serve as a three-dimensional potential trap by using a highly focused laser beam. The technique allows the non-invasive and remote manipulation of a microscopic particle without causing any thermal damage to the irradiated part of the samples.[2] So the optical tweezers have been a necessary tool in the study on the cell biology, especially on macromolecules. However, single optical tweezers cannot meet the needs of the manipulating of several cells at the same time. In recent years, the optical tweezers array has attracted much attention in the research of the technique. There have existed at least six kinds of methods to generate the optical trapping arrays, such as spatial light modulator,[3] diffractive optical element,[4] micro-chips,[5] micro-mirrors array, optical imaging fibre bundles,[6] and Fresnel biprisms interference.[7] The optical tweezers array has been used to sort the particles, such as the cells, by the researchers of interdisciplines.

The effort in this paper is made mainly to perform the theoretical analysis of gradient laser fields produced by interference beams. The interference field is generated by two identical plane shear interferometers to serve as the optical tweezers array. According to the theoretical analysis of gradient laser fields, we carry out the theoretical study of the trapping efficiency of an optical tweezers array system acting on spherical polystyrene particles.

For this trap system we perform force measurements by using the viscous drag exerted by fluid flow (Stokes' law), and we also describe the analysis of using trap stiffness to represent particle velocity to determine the behaviour of particles at different laser powers. The distribution of particles in the interference field is dependent on the parameters related to the gradient force, such as the size and refraction index of particle, the distribution of light field, the refraction index and the viscidity of liquid, etc. These parameters are discussed in detail and simulated by the Matlab software to show the influence of each parameter on the distribution of particle concentration.

*Project supported by the National Natural Science Foundation of China (Grant No 20505002), the Excellent Young Scholars Research Fund of Beijing Institute of Technology (Grant No 000Y06-23), and the Excellent Scholars Research Fund of Beijing (Grant No 20071D1600300394).
†E-mail: liqin70@bit.edu.cn

The spatial redistribution of particles in a laser interference field can also be predicted according to the theoretical analysis.

2. Gradient force

2.1. Background and concept of gradient force

The gradient interference fields responsible for potential trap usually can be focused by microscope objective. If we assume the light propagation direction to be along the axis, the distribution of the potential trap will be axisymmetrical. If we divide the coordinate system into transverse direction (perpendicular to the light propagation direction) and axial direction (along the light propagation direction), the status of particles is mainly determined by the transverse potential trap. In this paper, we mainly analyse the distribution of the particles in the transverse potential trap.

The particles located in a light field with a spatial gradient intensity, in the transverse potential trap along the one-dimensional x-axis of transverse plane are subjected to the action of the gradient dipole force F_{grad} along this axis. The results deducted in the following are based on the assumption that all vectors are represented by their magnitudes. If the calculated magnitude is positive, its corresponding vector points to the positive direction of the axis, and to the opposite direction in the case of negative magnitude. This force, i.e. F_{grad}, originates from the interaction between the light-induced dipole moment of a particle and the electrical component of light, and it is expressed as

$$F_{\mathrm{grad}} = \frac{\partial U}{\partial x}, \tag{1}$$

where

$$U = (pE) \tag{2}$$

is the energy of the dipole interaction, with

$$p = \alpha V E \tag{3}$$

being the induced dipole moment of the particle,

$$E = E_0 \cos(\omega t - kx) \tag{4}$$

being the electrical field strength, V being the particle volume. The results deducted in the following are based on the assumption that all particles are standard spherical particles. And

$$\alpha = 3n_{\mathrm{m}}^2 \frac{m^2 - 1}{m^2 + 2} \tag{5}$$

is the specific polarizability, where $m = n_{\mathrm{p}}/\ n_{\mathrm{m}}$ is the relative refractive index of the particle (n_{p} and n_{m} are the refractive indices of the particle and the surrounding medium).

Substituting expressions (2)–(4) into expression (1), and then averaging over the light oscillation period yield the gradient dipole force as follows:

$$F_{\mathrm{grad}} = \left(\frac{2\pi}{3}\right)\alpha r^3 \mathrm{grad}(E^2), \tag{6}$$

where r is the particle radius.

Thus, the gradient dipole force (referred to as the 'gradient force' hereafter) is directly proportional to the specific polarizability of the substance of which the particle is composed, the volume of the particle, and the light intensity gradient. This formula is only qualitative. The detailed analysis of each parameter will be expatiated in the following paragraph.

2.2. Gradient force in interference field

Along the x-axis of the transverse plane, the spatial modulation of light intensity can be achieved by the interfering of two identical plane waves each with amplitude E_1, intersecting at an angle 2β between the planes. In this case, the time-averaged total field E in the interference zone becomes modulated in the one-dimensional transverse x-direction (Here $\overline{E}$ instead of E is used for the averaging over the light oscillation period), and its squared value is

$$\overline{E}^2 = 2E_1^2\left\{1 + \cos\left(\frac{2\pi x}{x_0}\right)\right\}, \tag{7}$$

where the spatial period of the interference field is

$$x_0 = \frac{\lambda}{2n\beta} \tag{8}$$

with n being the index of the medium, β denoting half the angle between the planes, λ representing the wavelength of light and being taken as 632.8nm in our experimental instrument.

Substituting E^2 in expression (6) by $\overline{E}^2$ and according to the relation between the field strength and the intensity of the light beam $I_1 = \sqrt{\varepsilon/\mu}E_1^2$, and then averaging over the light oscillation period yield

the gradient force along the x-direction in the interference zone of two laser beams with the same intensity I_1 as follows:

$$F_{\text{grad}} = -\frac{8\pi^2 r^3}{3x_0}\alpha I_1 \sqrt{\frac{\mu}{\varepsilon}} \sin\left(\frac{2\pi x}{x_0}\right), \tag{9}$$

where ε and μ are the dielectric constant and magnetic conductivity respectively.

Expression (9) indicates that the gradient force is related to the parameters of the particles, viz radius r, specific polarizability α, dielectric constant ε, the magnetic conductivity μ, intensity of light beam I_1 and spatial period of the interference field x_0. The gradient force can cause the spatial redistribution and modulation of particles concentration in the focal plane of gradient interference fields focused by microscope objective.

3. Viscoelastic resistance

In general, biological samples, for example, cells or macromolecules, are on the order of microns in size. So they can be treated as Brown particles. When gradient forces capture the particles and move them in liquid, the viscoelasticity of liquid must attach viscoelastic resistance to the cell movement. According to the Navier-Stokes equation[8] in hydrokinetics, a particle is subjected to the action of the viscoelastic resistance of the liquid, F_{stockes}

$$F_{\text{stockes}} = 6\pi r\eta\nu, \tag{10}$$

where r is the particle radius, η is the viscoelastic coefficient of liquid, and ν is the velocity of particles.

3.1. The constant viscoelastic resistance

In the x-direction and y-direction interference fields, after their reaching an equilibrium state in which particles are trapped by the gradient force, the sample can be initially moved by a continuous system motor at a given constant velocity in the direction perpendicular to the optical axis of the microscope objective in order to stimulate a fluid flow. So this viscoelasticity of liquid must attach a constant viscoelastic resistance F_{constant} to the cell movement, therefore

$$F_{\text{constant}} = 6\pi r\eta\nu, \tag{11}$$

where r is the particle radius, η is the viscoelastic coefficient of liquid, and ν is the constant moving speed of particles given by the system motor.

3.2. The variable viscoelastic resistance

After the system motor has started to move the particles at a given initial speed v, the particles gain speeds of their own which will gradually increase. So these particle variable speeds must attach a variable viscoelastic resistance F_{variable} to the cell movement.

Among the analyses of all the parameters, the analysis of the variable velocity of particle is the most complex. So we use trap stiffness k and displacement $x(v)$ of the particles to represent the effect of particle velocity in determining the behaviour of particles. In fact, this trap stiffness k and displacement $x(v)$ can provide a direct measure of the restoring trapping force acting on the bead, and we can use them to represent the effect of particle velocity, i.e.

$$F_{\text{variable}} = 6\pi r\eta\nu = kx(v), \tag{12}$$

where k is the stiffness, and $x(v)$ is the displacement of the trapped particles from the equilibrium position.

4. Trap stiffness

The displacement of the trapped object from the centre of the trap under the action of an applied viscous fluid force usually can be monitored by using a position sensitive detector. It is determined by the spring (elastic) constant, i.e. the stiffness k of the optical trap

$$k = \frac{Q_{\text{t}} n_0}{x_{\max} c} P, \tag{13}$$

where Q_{t} is the trapping efficiency of the optical array system, c is the speed of light in vacuum, P is the radiant laser power, $x_{\max}$ is the maximum displacement of the particles from the equilibrium position, and n_0 is the water refractive index (usually n_0=1.33 at room temperature).

Obviously, stiffness k scales linearly with the laser power in the optical trap. The displacement $x(v)$ of the trapped particle from the equilibrium position (the central interference stripe) is a function of the viscous drag speed v below the critical speed v_{c}. Since the maximum displacement $x_{\max}$ is achieved at $v = v_{\text{c}}$ which corresponds to the maximum force of the trap, an optical tweezers array system is usually characterized in terms of the optical potential well by measuring the displacement of trapped particles undergoing a viscoelastic resistance with respect to fluid flowing at a speed below the critical speed. It is necessary to measure the optical trap stiffness before investigating very small forces such as those in biological processes.

5. Trapping efficiency

The trapping efficiency of the optical array system is usually described in terms of a dimensionless parameter Q_t, defined as the ratio between force F and the total momentum transferred by the laser beam (Pn_0/c).[9] It represents the fraction of momentum transferred to the trapping force from the trapping laser beam, i.e.

$$Q_t = \frac{Fc}{Pn_0}, \tag{14}$$

where c is the speed of light in vacuum, P is the laser power impinging on the bead and n_0 is the water refractive index (usually n_0=1.33 at room temperature).

6. Experimental setup

Our laser source is a semiconductor laser emitting at λ=532nm at room temperature. At this wavelength water exhibits a relative minimum in absorption spectrum which represents an important advantage for the non-invasive manipulation of biological particles. The laser beam is tightly focused onto a spot by using a 40× (NA=0.65) or a 100× (NA=1.25) objective lens to make the spatial period of the interference field x_0 reach 20μm. The trapped particles are polystyrene microspheres (ρ=1.06g/cm^3, n_p=1.65) with radii of 1, 2.5, 4, and 5μm.

The viscous force is balanced by the radial optical trap till the fluid speed reaches a critical speed v_c at which the particle escapes from the potential well created by the laser light. The critical speed of the trapped particle scales linearly with the laser power in the optical trap. Therefore, the maximum radial trapping force can be easily derived by measuring the critical speed where the trapping is no more active. The moment that the gradient forces of the interference field trap the particles, the equilibrium position is reached, at the point the viscous drag is balanced by the axial gradient force.[10]

Figure 1 shows the behaviour of the radii force against the laser power measured for polystyrene beads with radii between 1 and 5μm according to expression (9), subfigure (a) and (b) are for the cases of 40× and 100× microscope objectives, respectively.

As can be seen that the force varies between 0.2 and 35pN when the impinging laser power increases from 2 to 80mW. From the calculations of trapping force shown in Fig.1, we can find that the transverse force of the interference field is easy to capture the particles with a diameter (r=5μm) close to half the width (10μm) of the spatial period of the interference field (particles with other diameters receive lower trapping forces), and the increasing of the intensity of the interference field will strengthen the response of the particles to the field.

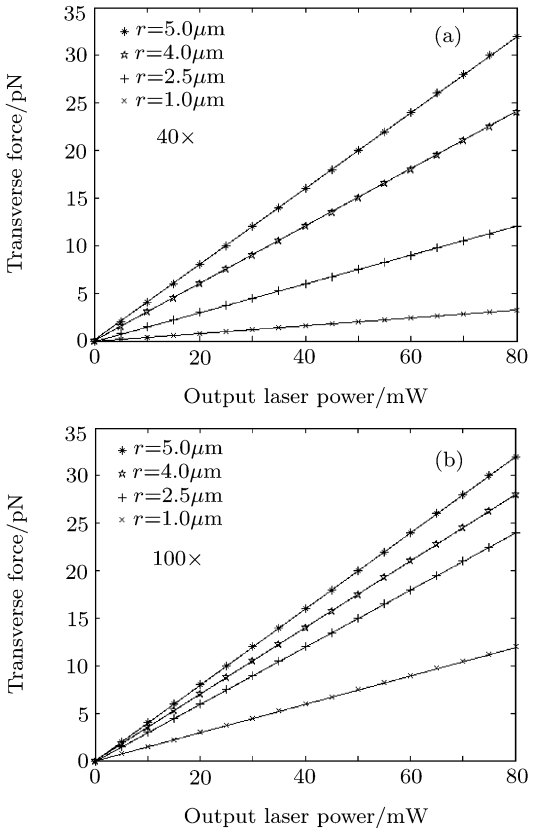


Fig.1. Transverse forces for different bead diameters, obtained with 40× (a) and 100× (b) objectives, respectively.

Then we apply the slopes of straight lines in Fig.1 to expression (14) to obtain the radial trap efficiency Q_t. The trap efficiencies are plotted in Fig.2 where the uncertainty is around 1.5% in fitting.

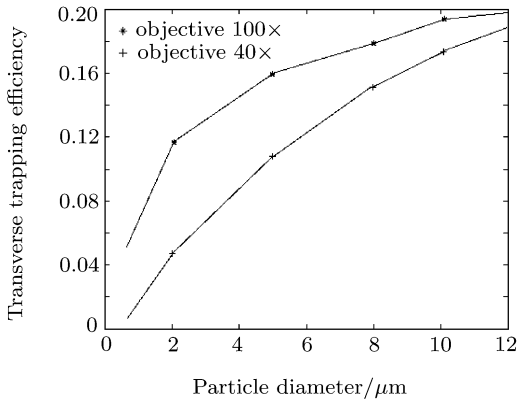


Fig.2. Behaviours of the transverse efficiency Q_t for the cases of 40× and 100× microscope objectives.

As can be seen for the cases of 40× and 100× objectives, the efficiency increases with the bead diameter increasing. In fact, for particles with $d > \lambda$, the trap efficiency is fully governed by ray-optics description which is independent of particle size. In addition, the 100× objective is more effective than the 40× one, for higher numerical aperture lenses can produce rays impinging on the trapped particles at larger incident angles. The radial force is directly proportional to laser power. In Mie regime ($d \ll \lambda$), the trapping axial force is independent of bead diameter, and it increases with aperture angle of the focused laser beam increasing. Therefore an efficient trap is accomplished when laser beams are highly focused by using high numerical aperture (NA) microscope objectives. Possible values of Q_{t} range between 0 and 1. Optical tweezers array configurations can be assessed experimentally to determine the values of trap efficiency Q_{t} in the lateral and axial directions separately.

Our results are reasonable qualitative results, but some discrepancies can be found when our results are compared with theoretical calculations or other different experimental measurements. The difference in experimental data among force measurements can be ascribed to several experimental parameters which are hard to be taken into account appropriately. One of them is the optical quality of the microscope objective lens system. Spherical aberration is particularly important for microscope objectives.

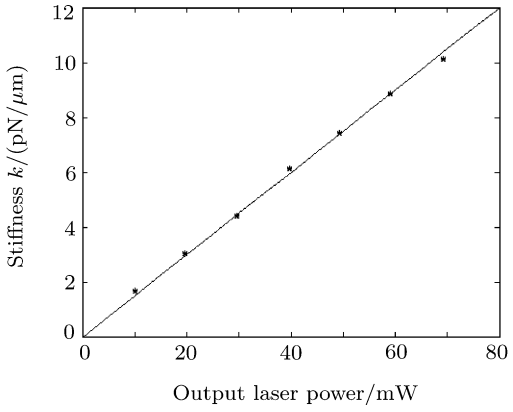


Fig.3. Trap stiffness k versus laser power for a polystyrene bead with the diameter d=10μm.

The values of k are estimated by fitting the experimental measurements and the obtained values against laser power are plotted in Fig.3. The stiffness k scales linearly with laser power in the optical trap. And the linear behaviour shown in Fig.3 can be easily understood if we compare the stiffness with the trap efficiency. Usually, trap stiffness tends to be in a range from 0.001 to 1pNnm^{-1}, depending on application conditions.

Displacement measurements can be then related to the optical potential energy of the trap through the well-known relation

$$U(x) = \frac{1}{2}kx^2 = \frac{1}{2}fx. \tag{15}$$

Potential energy results from position or configuration. A particle may have the capacity for escaping from the potential well due to its position in the gradient field, in other words, the optical potential energy.[11]

In our system displacement $x(v)$ is determined by the distance from the trapped interference stripe in Fig.4(a). Displacement $x(v)$ of the particle trapped from the equilibrium position is a function of the viscous drag speed v below the critical speed v_{c}. The parabolic curves of particle potential energy in Fig.4(b) show that the farther the particle is from the central equilibrium position, the larger its speed v is, and the higher its potential energy is.

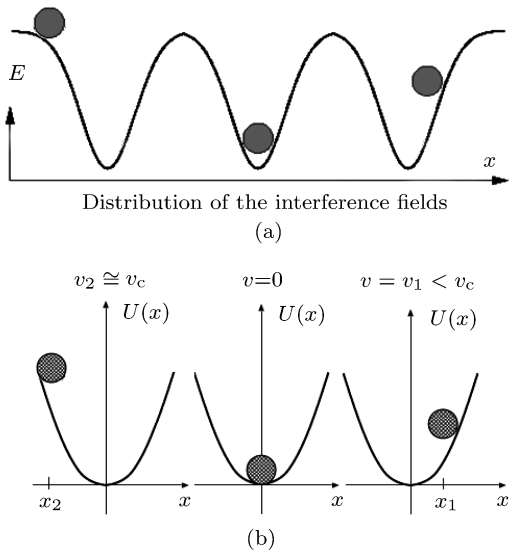


Fig.4. The optical potential energy related to displacement measurement. The middle case corresponds to the situation where the particle is trapped at the bottom of the potential well of the interference stripe. In the right and left cases, the drag force is active and it produces displacements x_1 and x_2 from the equilibrium position, corresponding to two different fluid speeds v_1 and v_2.

Figure 5 shows that typical potential curves $U(x)$ versus displacement of a polystyrene bead with a 10μm diameter at different laser powers. We can see that the higher the laser power is, the more concen-

trated the potential energy curves are.

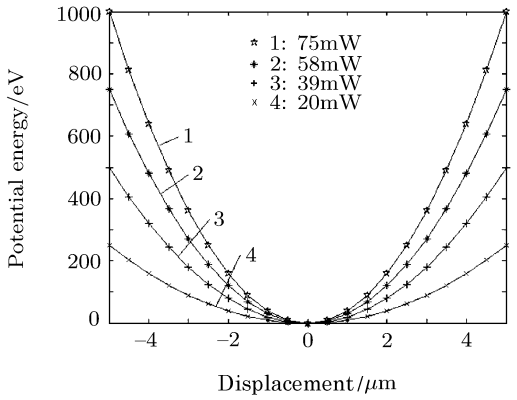


Fig.5. Behaviours of the potential wells of optical trap, obtained with a 40x objective lens at different laser powers for a polystyrene bead (d=10μm).

7. Simulation model

7.1. The resultant force on a particle

In our system, after the particles have been trapped, when gradient forces capture the particles and move them in liquid (from centre to the two sides), the particles will receive gradient force and viscoelastic resistance which includes both the constant viscoelastic resistance in expression (11) caused by a given constant initial speed v of the system motor and the variable viscoelastic resistance in expression (12) caused by the variable speeds of particle's own.

Because we are concerned only about the distribution of the particles in the transverse potential trap, the gradient force of the interference field and the viscoelastic resistance of the liquid have opposite effects on the particles (in opposite directions). When gradient forces make a particle move, the resultant force F acting on it is

$$\begin{aligned} F =& F_{\text{grad}} - F_{\text{stockes}} = F_{\text{grad}} - F_{\text{constant}} - F_{\text{variable}} \\ =& \frac{8\pi^2 r^3}{3x_0}\alpha I_1 \sqrt{\frac{\mu}{\varepsilon}} \sin\left(\frac{2\pi x}{x_0}\right) \\ & - 6\pi r\eta\nu - kx. \end{aligned} \tag{16}$$

7.2. The spatial distribution of particle concentration

The interaction between the gradient force and the viscoelastic resistance causes a spatial redistribution of particle concentration, $n(x,t)$, in the liquid. The magnitude of $n(x,t)$ is directly proportional to the force acting on the particles.

The evolution of $n(x,t)$ is determined by the one-dimensional Planck-Nernst equation, which describes the motion of particles under the action of an external force, with the hydrodynamic friction taken into consideration, as follows:

$$\alpha\frac{\partial n}{\partial t} = D\frac{\partial^2 n}{\partial x^2} - b\frac{\partial}{\partial x}(nF), \tag{17}$$

where, D is the diffusion coefficient and b is the coefficient of mobility.

Diffusion coefficient D is related to mobility b by the Einstein formula $D = KTb$, where K is the Boltzmann constant and T is the temperature. The right-hand side of Eq.(17) contains two terms: the first term is responsible for the diffusion current and the second term for the current induced by the resultant force F in expression (16). Let the terms on the right-hand side of Eq.(17) equal zero, then, for the cases under consideration, we will be able to find each steady-state solution of the Planck-Nernst equation in the gripping and moving processes in the transverse potential trap. In each steady state, particles are subjected to not only the gradient force, but also the viscoelastic resistance. Therefore,

$$\begin{aligned} n(x) =& B_1 n_0 \exp\left\{\frac{4\pi\alpha r^3}{3KT} I_1 \sqrt{\frac{\mu}{\varepsilon}} \cos\left(\frac{2\pi x}{x_0}\right)\right. \\ & \left. - \frac{k}{2KT}x^2 - \frac{6\pi r\eta\nu}{KT}x\right\}, \end{aligned} \tag{18}$$

where $n(x)$ is the spatial distribution of particle concentration in the x-direction; n_0 is the initial particle concentration in the system; α is the specific polarizability, related to the refractive indices of the particles and the surrounding medium (generally speaking, the larger the refractive index of particles is, the higher the particles density will be, so the refractive index is often referred to as the density); r is the particle radius; k is the trap stiffness; K is the Boltzmann constant; T is the temperature; I_1 is the intensity of the laser beam in units of lumen/solid angle; x_0 is the spatial period of the interference field in the x-direction; ε is the dielectric constant; μ is the magnetic conductivity (often using the magnetic conductivity in vacuum, μ_0=4$\pi\times10^{-7}$Hm^{-1}); η is the viscoelastic coefficient of liquid; ν is the speed of particles; The normalization factor B_1 is determined from the condition of conservation of the total number of particles in the modula-

tion period in the x-direction

$$\int_0^{x_0} n(x)\mathrm{d}x = n_0 x_0, \tag{19}$$

From the above results, we obtain the spatial distribution of particles with different sizes, densities, refraction indices and dielectric constants during moving in the one-dimensional transverse potential trap.

Expression (18) describes the effect of each parameter on the spatial distribution of the particles in the x-direction. In the following, several important parameters are discussed in detail and simulated by the Matlab software to show the influence of each parameter in the expression.

The simulated results are based on the following assumption: the spatial period of the interference field x_0 is 20μm; the centre of the interference fields corresponds to the zero-level stripe, and the model is established for the process in which gradient forces capture the particles and move them in the transverse focal plane; the horizontal axis of the figures represents the period number (x/x_0), and the vertical axis represents the relative spatial modulation of particles ($n(x)/n_0$).

7.3. Particles size r

We analyse the first important parameter in expression (18), particle radius r, to show its influence on the spatial modulation of particle concentration. Figure 6 indicates the responses of components at different values of radius r: 1, 2.5 and 5μm, to the interference field.

For convenience, we use the power density of two interference beams, E_1 (in units of W·cm^{-2}), to replace I_1 in expression (18). E_1 and I_1 are related by

$$E_1 \times S \times K(\lambda)/2\pi = I_1, \tag{20}$$

where λ=532nm, $K(\lambda)$=683×$V(\lambda)$, and S is the irradiation area of the laser field. Here we have used quite a moderate light intensity E_1=0.6W·cm^{-2}, S=50mm^2, the refraction index of the polymeric balls n_p=1.65 and the refraction index of the liquid n_m=1. Substituting the parameters into expression (18), we can obtain the theoretical curves for the relative spatial modulation of concentration for the particles with different radii. For the case of η=8.935×10^{-6}Pa·s, as the spatial period of the interference field x_0 is 20μm, we can find that particles of 5μm radius respond to the field most obviously. Particles of 1μm and 2.5μm radii just slightly respond to the interference field. The result shows that the interference field is easy to capture the particles with a diameter close to half the width of the spatial period of the interference field. This result is in agreement with the theoretical one of trap efficiency Q_t, as briefly mentioned above. The spatial distribution of particle concentration is subjected to the negative effect of the viscoelastic resistance caused by both an initial speed v given by the system motor and the variable speed of the particles, and it will be modulated by the difference between the gradient force and the viscoelastic resistance.

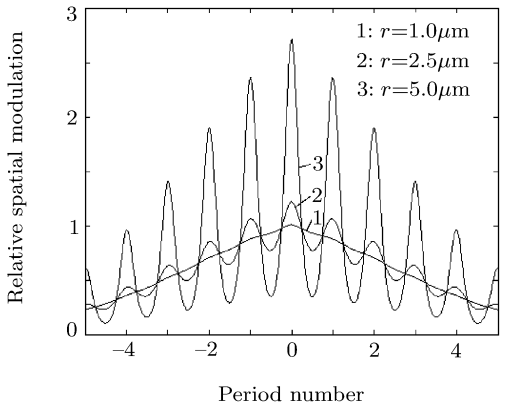


Fig.6. The responses of components of different radii, 1μm(Curve 1), 2.5μm(Curve 2) and 5μm(Curve 3), to the 20μm spatial period of the interference field, with each of two interference beams having a power density of 0.6W·cm^{-2}.

7.4. Laser beams intensity I_1

We analyse the second important parameter I_1 in expression (15) to show its influence on the spatial modulation of particle concentration. Since I_1 is directly proportional to E_1, we increase the power densities of two interference beams to E_1=3W·cm^{-2}; the other parameters used in simulation are S=50mm^2, the refraction index of the polymeric balls n_p=1.6 and the refraction index of the liquid n_m=1. For the case of η=8.935×10^{-6}Pa·s, Figure 7 indicates the responses of components with different radii: 1, 2.5 and 5μm, to the same interference field. Comparing the amplitude of the relative spatial modulation in Figure 6 with that in Fig.7, it is obvious that the increasing of the interference field intensity will strengthen the response of the particles to the field and the spatial modulation of particle concentration will also increase. This result is in agreement with the theoretical one of stiffness k, as briefly mentioned above.

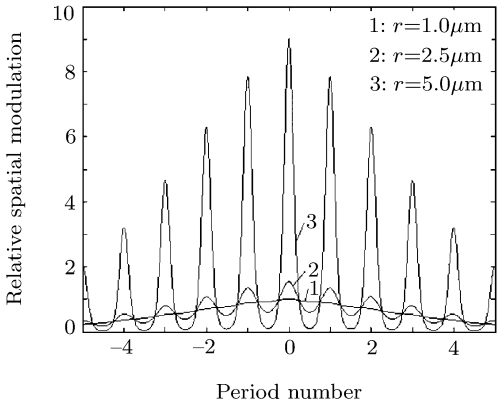


Fig.7. The responses of components with different radii, 1μm(Curve 1), 2.5μm(Curve 2) and 5μm(Curve 3), to the 20μm spatial period of the interference field, with each of two interference beams having a power density of 3W·cm^{-2}.

7.5. Specific polarizability of particle α

The third important parameter in expression (18) is the specific polarizability of the particle α, which is related to the refractive indices of the particle and the surrounding medium. We also use the power density of two interference beams E_1 to replace I_1. λ, $K(\lambda)$, S are the same as those before in value. Here we use the following parameter values: η=8.935×10^{-6}Pa·s, E_1=4W·cm^{-2}, r=5μm, the refraction index of the polymeric balls $n_{\rm p1}$=1.6, the refraction index of the air bubbles $n_{\rm p2}$=0.6, and the refraction index of the liquid $n_{\rm m}$=1. Substituting these parameter values into expression (18), we can obtain the theoretical curves for the relative spatial modulation of polymeric balls (curve 1) and air bubbles (curve 2). Curve 3 shows their distribution without any interference field existing.

Figure 8 shows that, in the case of $\alpha > 0$ (when $n_{\rm p} > n_{\rm m}$), such as polymeric balls in water solutions, the force is along the field gradient direction. So the balls distribute at the centre of the bright strip. On the other hand, in the case of $\alpha < 0$ (when $n_{\rm p} < n_{\rm m}$), such as air bubbles in water solutions, the force is along the direction opposite to that of the field gradient. So air bubbles distribute around the dark strip. Generally speaking, the larger the refractive index of the particles is, the higher the particle density will be. Therefore, refractive index is often referred to as the density. This means that the particles with a larger density than that of the surrounding medium will be pulled into the region of the field maximum, while the less dense particles will be pushed out of this region.

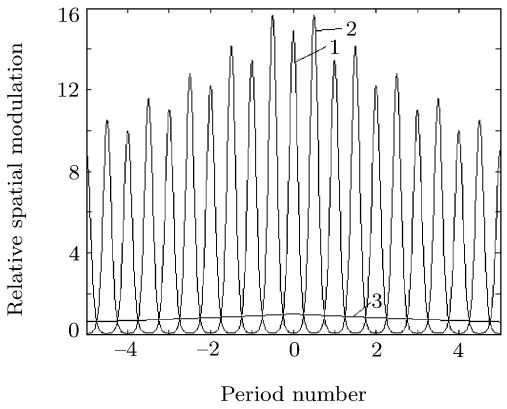


Fig.8. The responses of components at specific polarizabilities of different particles: polymeric balls (Curve 1) and air bubbles (Curve 2), to the spatial period of the interference field, with each of two interference beams having a power density of 4W·cm^{-2} and curve 3 showing their distribution without any interference field existing.

7.6. Viscoelastic coefficient η

The fourth important parameter in expression (18) is the viscoelastic coefficient η. $\lambda, K(\lambda)$, S are the same as those before in value. Here the following parameter values are used: η=8.935×10^{-6}Pa·s, E_1=0.6W·cm^{-2}, r=5μm, the refraction index of the polymeric balls $n_{\rm p1}$=1.6, and the refraction index of the liquid $n_{\rm m}$=1. Substituting these parameter values into expression (18), we can obtain the theoretical curves at different values of viscoelastic coefficient η for the relative spatial modulation of particle concentration in Fig.9.

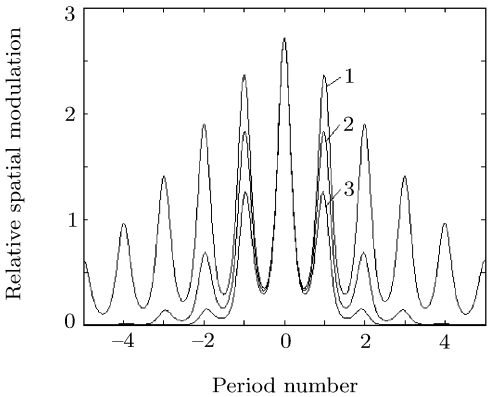


Fig.9. The effect of viscoelastic coefficient of liquid on the spatial modulation of particles (Curve 1: η = 8.935×10^{-6}Pa·s, Curve 2: η = 2.139×10^{-4}Pa·s, Curve 3: η = 1.655×10^{-3}Pa·s)

Clearly, when gradient forces capture the particles and move them in a transverse focal plane, the negative

effects of different values of viscoelastic resistance on particles are different. The larger the viscoelastic coefficient is, the more obvious the negative effect on the spatial modulation of particle concentration will be.

The above simulation results demonstrate the relationship between the relative spatial modulation of particle concentration and particle radius r, laser beams intensity I_1, specific polarizability of particles α, and viscoelastic coefficient η. According to these relationships, the sample can be sorted by changing appropriate parameters. This is the theoretical principle of the corresponding instrument design.

7.7. Model of optical tweezers array

According to the above analyses, we can set up an optical tweezers array by using two interference fields with identical power densities, overlapping at a certain angle.

In the y-direction of the transverse focal plane, the spatial distribution of particles during their moving can also be obtained by using the same method

$$n(y) = B_2 n_0 \exp\left\{\frac{4\pi\alpha r^3}{3KT} I_1 \sqrt{\frac{\mu}{\varepsilon}} \cos\left(\frac{2\pi y}{y_0}\right) - \frac{k}{2KT} y^2 - \frac{6\pi r\eta\nu}{KT} y\right\}, \tag{21}$$

where $n(y)$ is the spatial distribution of particles in the y-direction; y_0 is the spatial period of the interference field in the y-direction; the normalization factor B_2 is determined by the condition of conservation of the total number of particles in the modulation period in the y-direction

$$\int_0^{y_0} n(y)\mathrm{d}y = n_0 y_0, \tag{22}$$

The meanings of the other parameters in expression (21) are the same as those in expression (18). Obviously, in the y-direction of the transverse focal plane, the simulation results of the spatial distribution of particles are the same as the results in the x-direction.

If we choose the overlapping angle as 90°, η=2.139×10^{-4}Pa·s, and the other parameters to be not changed, the simulation of the optical tweezers array in the focal plane is shown in Fig.10. The spatial redistribution of particles is shifted from the centre to the surrounding area in the transverse focal plane, implying that the spatial redistribution of particles is affected by the negative effect of the viscoelastic resistance caused by both an initial speed v given by the system motor and the variable speeds of particles, and this effect gradually declines.

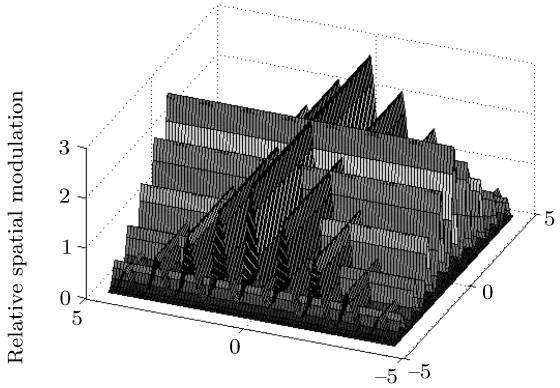


Fig.10. The simulation model of the optical tweezers array.

8. Discussion and conclusion

In this paper, we have made the theoretical analysis on an optical tweezers array system based on a semiconductor laser (λ =532nm) in a power range of 2–80mW. Our system is used for trapping polystyrene spheres with diameters ranging from 1 to 10μm by using 40× and 100× microscope objectives. We have realized a simple and effective method to investigate the speed of particles in the optical potential well based on the measurements of displacement of the trapped particle from the equilibrium position when the fluid flow speed is below the escaping speed v_c. Moreover we have observed that high NA objectives can give a high trapping efficiency. In addition, we have discussed the theoretical principle of an optical tweezers array by using two interference fields with identical power densities, overlapping at a certain angle. The gradient force action caused by the interference laser light may significantly influence the path and speed of the sorting processes.

There are also other ways to obtain the best focused image and improve the tapping efficiency. For example, an optical tweezers array system can also be placed under quadrant position sensitive detector (PSD) feedback control so that any particle movement out of an equilibrium position can be immediately corrected by the repositioning of the trap itself, so that the particle remains stationary within the trap.[12] The using of Laguerre-Gaussian (LG) beams can also increase the axial trapping efficiency, but the scattering force reduces.[13]

An optical tweezers array system can realize noncontact operation. So such a mechanism can be ap-

plied to separate and manipulate the living cells. The application of this method opens up possibilities for controlling fundamental biological processes and may offer new technologies in laser therapy.

References

[1] Ashkin A, Dziedzic J M, Bjorkholm J E and Chu S 1986 *Opt. Lett.* **11** 288

[2] Mehta A D, Rief M, Spudich J A, Smith D A and Simmons R M 1999 *Science* **283** 1689

[3] Rodrigo J P, Eriksen L R, Daria V R and Glückstad J 2002 *Opt. Express* **10** 1550

[4] Korda T P, Taylor B M and Grier G D 2002 *Phys. Rev. Lett.* **89** 128301

[5] Fu Y A, Spence1 C, Scherer A, Arnold H F and Quake R S 1999 *Nature Biotechnol.* **17** 1109

[6] Tam M J, Biran I and Walt R D 2004 *Appl. Phys. Lett.* **84** 4289

[7] Rubinov A N 2003 *J. Phys. D (Appl. Phys.)* **36** 2317

[8] Zhou H, Li X F, Li Y M, Lou L R and Y J C 2001 *Prog. Biochem. Biophys.* **28** 903

[9] Simpson N B, McGloin D, Dholakia K, Allen L and Padgett M J 1998 *J. Mod. Opt.* **45** 1943

[10] Gong Z, Chen H T, Li Y M, Lou L R and Qiu J 2005 *J. University of Science and Technology of China* **35** 601 (in Chinese)

[11] Neuman K C and Block S M 2004 *Rev. Sci. Instrum.* **75** 2787

[12] Xu S H, Li Y M and Lou L R 2006 *Chin. Phys.* **15** 1391

[13] Soni G V, Hameed F M, Roopa T and Shivashankar G V 2002 *Curr. Sci.* **83** 1464